Radar-Based Refractivity Maps Using Geostatistical Interpolation

Brais Sánchez-Rama, Rubén Nocelo López, Verónica Santalla del Río, *Member, IEEE,* and Timothy Darlington

***Abstract*—Tropospheric refractivity, which is closely related to temperature, pressure, and relative humidity, is a valuable parameter for weather forecasting and climate analysis. It has already been demonstrated that refractivity estimates can be derived using the phase measurements corresponding to radar signals backscattered from stationary targets over any terrain orography, with high temporal resolution. However, the random distribution of stationary targets affects the spatial resolution provided by the computed refractivity estimates. It is of interest to obtain reliable radar-based refractivity maps to assist final users with data interpretation and analysis, so the use of the a suitable geostatistical interpolation technique to obtain refractivity maps is studied in this paper. Refractivity estimates obtained from C-band radar data gathered during 2019 by the United Kingdom's national weather service (Met Office) are used to evaluate the accuracy of the method by comparing the results to ground-based weather stations and the ECMWF's ERA5 reanalysis dataset.**

***Index Terms*—Geostatistical interpolation, radar, atmospheric refractivity characterization.**

I. Introduction

THE tropospheric refractivity is an interesting parameter for the meteorological community given its close relation to temperature, pressure, and relative humidity. For instance, this parameter can be used for Numerical Weather Prediction (NWP) models in order to improve the weather forecasting [1], [2]. However, it has generally been acknowledged that the precision and accuracy of the tropospheric refractivity measurements obtained by existing methods in the lower troposphere are slightly poor, the automatic weather station networks that provide in situ measurements cannot achieve sufficient spatial resolution without increasing development and maintenance costs [3]. It is mainly just moisture that is currently observed [4]. On the other hand, the Radio Occultation (RO) technique provides refractivity measurements with high accuracy and high vertical resolution, but it is used more in the middle-upper part of the atmosphere than in the lower troposphere [5].

Since the radar-based refractivity estimation technique was proposed by [6], it has received special attention from the meteorological community due to its good performance when estimating tropospheric refractivity in the lower troposphere. This technique, based on radar phase measurements from stationary targets echoes [7], has been probed and validated over the years with radars operating at different frequency bands (S-Band [8], C-Band [9] and X-Band [10]) and using phased array radars [11]. Furthermore, this technique has been also validated for radars equipped with coherent klystron-based transmitter systems [8] and with magnetron-based transmitter systems [12], [13]. The potential of the radar-based refractivity measurements was also evaluated in different global experiments such as the IHOP_2002 [8], the Refractivity Experiment for H_20 Research and Collaborative Operational Technology Transfer (REFRACTT) [14] and the HyMeX campaign [3], where results showed a high correlation with refractivity measurements obtained from other instruments. Moreover, its application was demonstrated not only in flat areas [8] but also in hilly areas [15].

The radar-based refractivity estimation technique provides accurate estimates with high temporal resolution. However, it should be noted that the spatial resolution depends largely on the orography around the radar. When the identified stationary targets are scarce, the spatial resolution decreases. Different studies have considered the use of spatial averaging techniques to address this issue and help end-users with data visualisation, such as the 4-km pyramidal-like smoothing function proposed in [8], or the direct space average used in [3]. However, these techniques depend on the number of ground targets in the area, so gaps without refractivity values appear at locations without any stationary target.

The use of a suitable interpolation method would take advantage of the geospatial characteristics of the tropospheric refractivity, allowing for the generation of reliable refractivity maps even in locations with low target density. Among the different interpolation methods, the kriging interpolation technique, that provides the Best Linear Unbiased Predictor (BLUP) [16], [17], is studied in this paper. This approach leads to the possibility of achieving refractivity maps up to 50–60 km away from the radar, the maximum range at which stationary targets can be typically identified.

In Section II, the radar refractivity interpolation approach proposed in this paper is briefly reviewed. Section III describes the dataset and, finally, the achieved results and conclusions are discussed in Sections IV and V, respectively.

II. Radar Refractivity Interpolation

Radar refractivity estimates are derived from the phase of the radar signals backscattered from stationary targets. The method presented in [15] proposes to estimate the mean refractivity within a predefined area, $\overline{N}$, and the refractivity gradient, $\partial N/\partial h$, as the values that minimise a cost function

B. Sánchez-Rama and V. Santalla del Río are with the atlanTTic Research Center, Universidade de Vigo, 36310 Vigo, Spain. (e-mail: veronica@uvigo.es).

R. Nocelo López is with the Defense University Center at the Spanish Naval Academy, 36920 Marín, Spain.

T. Darlington is with the Met Office, Exeter, United Kingdom.

Manuscript received MONTH DAY, YEAR; revised MONTH DAY, YEAR.

directly related to the sum of the squares of the residuals of all stationary targets pairs identified within the area of interest (Equation (7) in [15]). For each stationary target pair, the residual is obtained as the difference between the measured phase difference between the two targets of the pair (e.g. $T0_k$ and $T1_k$) and the phase difference function of that pair, $\Delta\Phi_{T0_k,T1_k}(\overline{N}, \partial N/\partial h)$, previously estimated during the calibration period. The accuracy of the method is related to the density of stationary targets pairs within the area of calculation. Results in [15] show that, for areas between around 8×8 km^2 and 15×15 km^2, between 100 and 200 stationary targets pairs give reasonable accuracy.

Considering this, the radar coverage area can be divided into smaller areas wherein estimates of the refractivity can be obtained. These estimates are then interpolated to obtain the refractivity at any other point within the radar coverage area. This approach requires:

1) To define the smaller areas where the refractivity is going to be estimated from the radar measurements. During this study, a k-means clustering method has been used to group the identified targets.
2) The implementation of an spatial interpolation method. Geostatistical interpolation has been preferred over deterministic interpolation considering that the large amount of data provided by weather radars allows for a good statistical characterization and then, the use of the spatial correlation of the refractivity. Therefore, kriging methods have been considered. They are well-established and proven interpolation methods that, assuming second-order stationarity of the data, provide the Best Linear Unbiased Predictor (BLUP). Choosing one kriging method over another depends mainly on the knowledge or assumptions about the mean of the underlying process. Ordinary kriging provides estimates without requiring knowledge of the mean, which is usually unknown. On the other hand, universal kriging should be used if it is known that the data presents a spatial trend. The refractivity data derived from ERA-5 measurements [18], which will be later used for cross-validation as it is an independent and reliable data set, has been analysed and no spatial trend has been found in the coverage area of the radars considered in this study. In view of this, ordinary kriging has been chosen and implemented.

A. Kriging interpolation

The ordinary kriging predictor of a random function $Z(x)$ at point x, that has been observed at N locations, $x_i, i = 1, ..., N$, $\hat{Z}(x)$, is a weighted linear combination of the random function at the sampled locations:

$$\hat{Z}(x) = \sum_{i=1}^{N} \lambda_i Z(x_i) \tag{1}$$

The weights, λ_i, calculated to ensure the unbiasedness and minimum variance of the predictor, are a function of the semivariogram, $\gamma(x_i - x_j) = E\{(Z(x_i) - Z(x_j))^2\}/2$, that characterizes the spatial correlation of $Z(x)$ [16], [19]. In general, the semivariogram is not known and must be estimated from the data. Estimation of the variogram is a key point in kriging interpolation to ensure good accuracy of the results. During this study, the variogram models that are most used in the bibliograpy (e.g., gaussian, circular or spherical) have been evaluated. The obtained results show that the circular model fits well with the radar refractivity data available. The model parameters are estimated from the data of a radar scan for each interpolation. Figure 1 shows the model fitted to the experimental variogram data corresponding with consecutive radar scans performed on January 1st, 2019, between 01:15 and 01:35 UTC time.

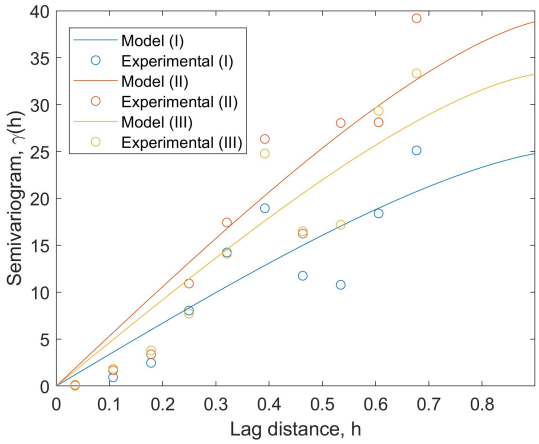

Fig. 1. Experimental semivariograms obtained from the refractivity estimates and fitted circular model.

III. Dataset description

Real radar measurements gathered during 2019 by the United Kingdom's national weather service (Met Office) [20] are used to test and analyse the kriging interpolation of radar refractivity data. In particular, data from Munduff and Holehead weather radars were chosen for the analysis. The close proximity of these two radars allows to combine their coverage areas to define a larger testing area (see Figure 2).

To collect the data, every 10 minutes, a dedicated 0^o elevation scan was performed in an attempt to maximize the ground clutter. Short pulses were used (0.5μs / 75m range resolution) to improve the phase measurement quality in relation to the error term which is picked up due to any offset of the target within the sample volume, as described in [13]. The final data consist of 1°, integrated, averaged phase values. To identify the stationary targets, considering that the data were already integrated, the Reliability Index (RI) proposed in [11] was used. Figure 2 presents the identified stationary targets within the area under test, and Figure 3 the obtained clusters.

The refractivity estimation algorithm [15] is run for each cluster and scan, so that a refractivity estimate per cluster and radar scan is obtained. Figure 4 shows, as an example, the refractivity estimates obtained from the scan performed on January 1st, 2019 at 14:15 UTC. The location of each

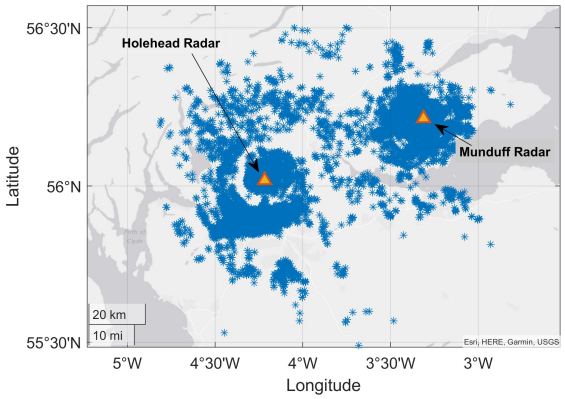

Fig. 2. Raw stationary targets identified within Holehead and Munduff's weather radar coverage areas.

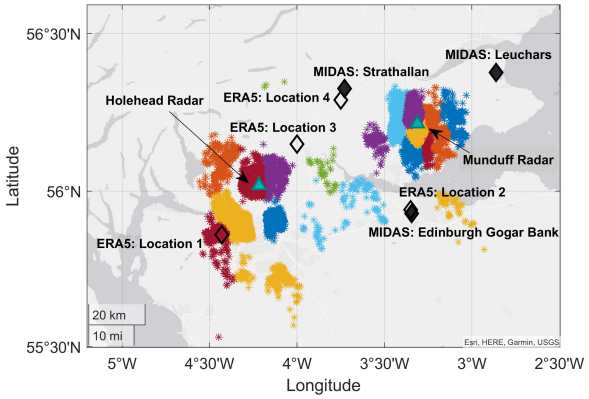

Fig. 3. Clusters of stationary targets identified within Holehead and Munduff's weather radar coverage areas. The locations of the ground-based weather stations and ERA5 grid points used to validate the accuracy of the interpolated refractivity maps are also shown.

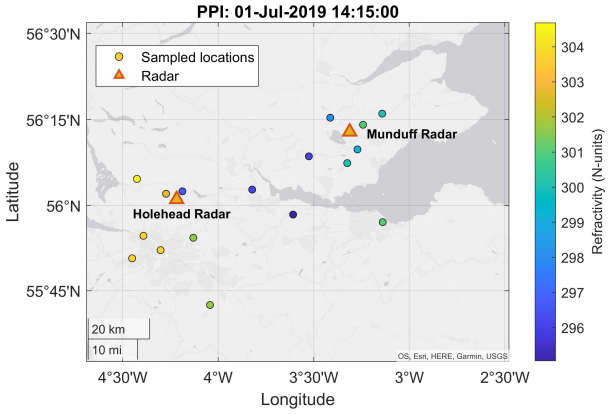

Fig. 4. Radar-based refractivity estimates obtained for each cluster corresponding to the scan performed on July 1st, 2019 at 14:15 UTC.

estimate corresponds with the centroid of its cluster, and the colour indicates the estimated refractivity value.

From the estimated refractivity samples, using ordinary kriging interpolation, refractivity maps for the joint coverage area of Munduff and Holehead radars are produced. Figure

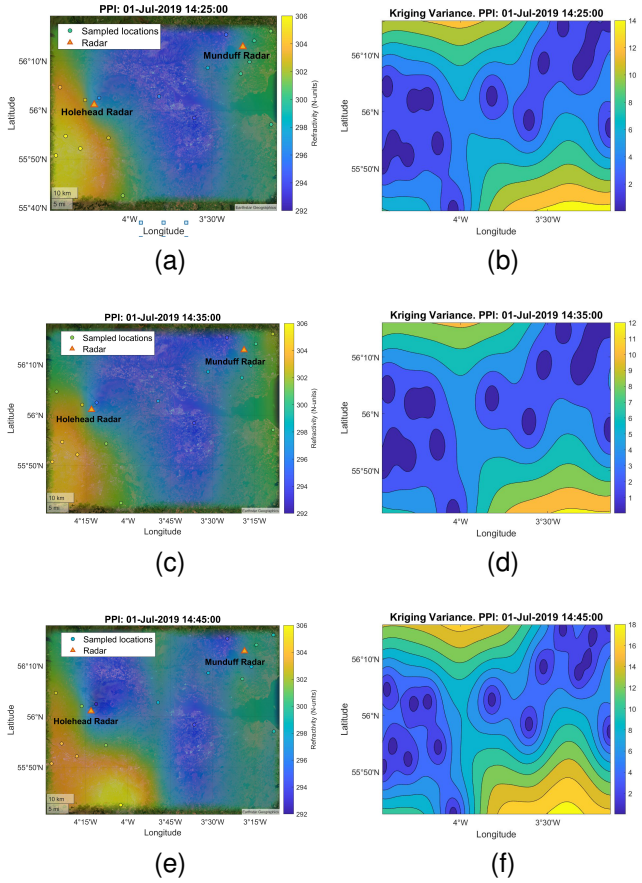

Fig. 5. Left column: Refractivity fields obtained using ordinary kriging. They correspond to consecutive radar scans performed on July 1st, 2019. Right column: Kriging prediction variance of the refractivity maps.

5(a)-(c)-(e) shows the kriging-derived refractivity maps calculated from three consecutive radar scans on July 1st, 2019.

IV. Results

The usual approach to assess the quality of kriging-based interpolation results relies on analysing the prediction variance, shown in Figure 5(b)-(d)-(f). However, the computation of the kriging variance does not consider any uncertainty source introduced by the radar-based refractivity estimation algorithm. Thus, refractivity data gathered from alternative sources will be compared to the produced kriging estimates in order to perform an end-to-end validation of the interpolated refractivity fields.

A. Validation using local ground-based weather stations

Data from three ground-based weather stations within the area under test [21] are used to validate the refractivity kriging estimates obtained from radar data. The location of the weather stations is shown in Figure 3. Hourly data of temperature, humidity and pressure from the weather stations are used to obtain hourly tropospheric refractivity at each one of the weather stations. The hourly data is linearly interpolated to obtain the refractivity at each radar scan time. For each radar scan the radar based refractivity map is calculated. Note that,

since the estimation algorithm also provides estimates of the refractivity vertical gradient [15], the height factor in the refractivity estimates can be compensated for. Therefore, the kriging-derived interpolated maps have been obtained at each ground station height, so the comparison is performed as objectively as possible.

Figure 6 shows the refractivity obtained at each weather station with the refractivity kriging predictor value obtained at the nearest interpolation grid point to each of the stations. It can be seen that, even though two of the three weather stations are located at a considerable distance from the nearest cluster, the accuracy of the interpolated values is quite reasonable according to the computed RMSE and Pearson correlation coefficient, ρ (see Table I).

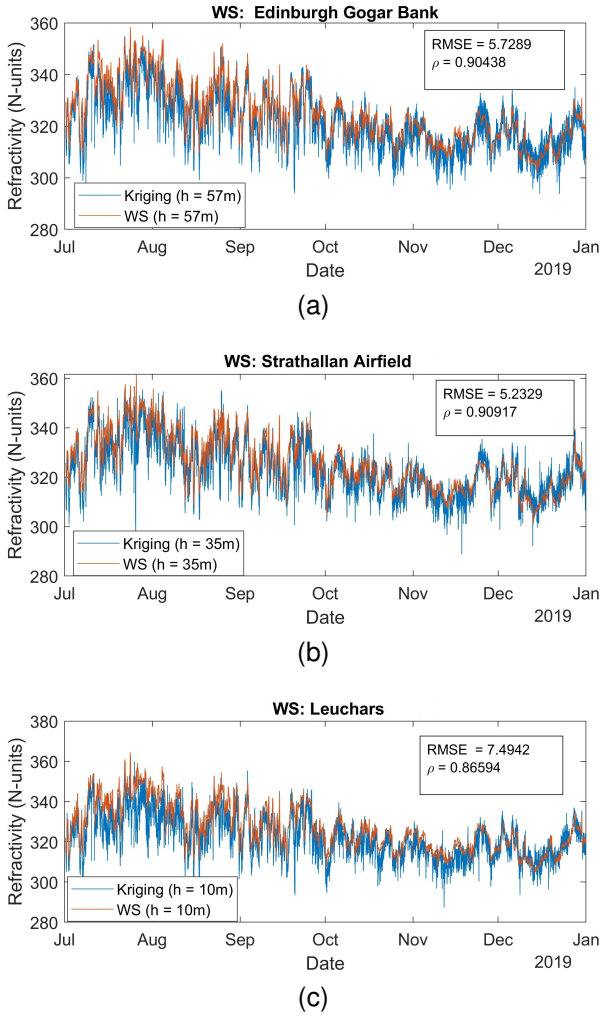

Fig. 6. Comparison of the refractivity calculated from ground-based weather stations data and the refractivity values from the nearest point in the radar-based interpolation grid.

B. Validation using the ERA5 reanalysis dataset

The ERA5 reanalysis dataset, generated using global multi-input NWP models, is provided by the European Centre for Medium-Range Weather Forecasts (ECMWF) [18]. Since ERA5 is obtained using data assimilation techniques, their accuracy and precision are enhanced by combining numerical model predictions with real observations. The hourly data resolve the atmosphere using 137 levels from the ground up to an altitude of 80 km, covering the Earth on a grid of 30 km.

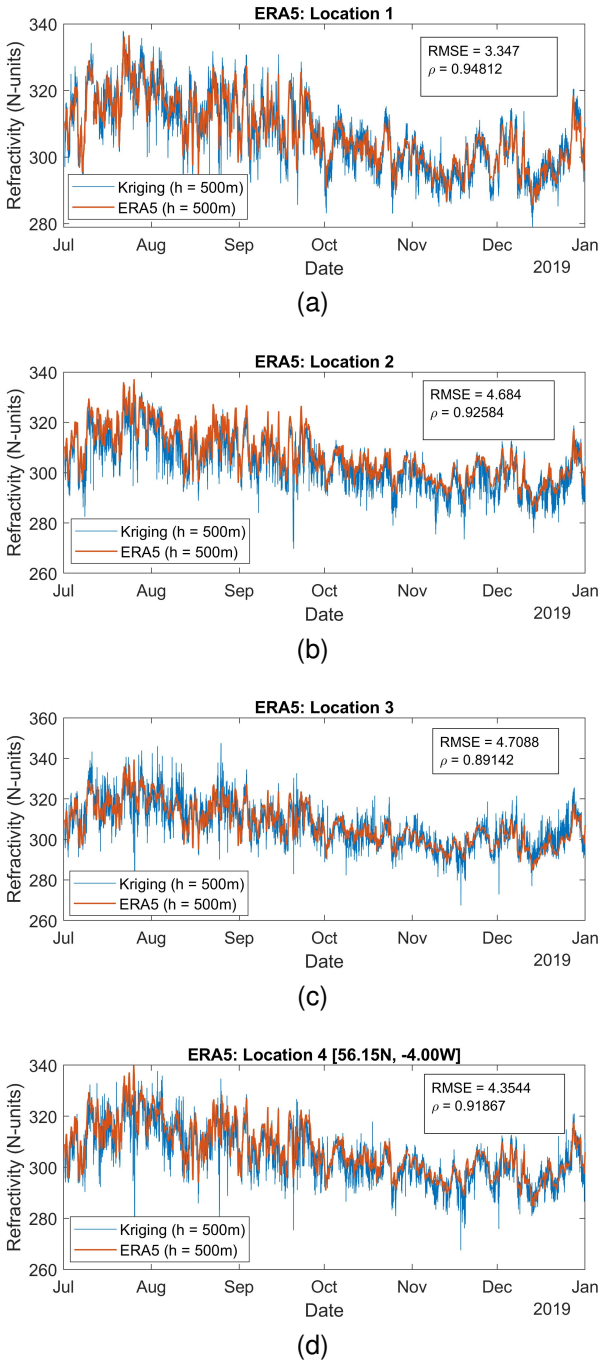

Fig. 7. Comparison of the refractivity calculated using the ERA5 reanalysis dataset and the refractivity values from the nearest point in the radar-based interpolation grid.

Four different locations, shown in Figure 3, were chosen. Similarly to the validation process based on weather stations, hourly refractivity estimates calculated from ERA5-derived temperature, humidity and pressure data, were linearly interpolated to obtain refractivity estimates at the radar scan times, and these were compared to the kriging interpolated values at the chosen locations. Figure 7 shows the ERA5 based

refractivity at each ERA5 chosen spot and the refractivity kriging prediction at the nearest interpolation grid point. In order to perform a fair comparison (which is summarised in Table I), the refractivity maps were generated considering a height of 500 m above sea level, which is, approximately, the average altitude between both radars

TABLE I
SUMMARY OF THE KRIGING EVALUATION RESULTS OBTAINED WITHIN HOLEHEAD AND MUNDUFF'S WEATHER RADAR COVERAGE AREAS.

Location	**Reference Source**	**RMSE**	ρ
Edinburgh Gogar Bank	WS	5.7289	0.9044
Strathallan Airfield	WS	5.2329	0.9092
Leuchars	WS	7.4942	0.8659
Location 1	ERA5	3.3470	0.9481
Location 2	ERA5	4.6840	0.9258
Location 3	ERA5	4.7088	0.8914
Location 4	ERA5	4.3544	0.9187

V. CONCLUSIONS

In this paper, the feasibility of using ordinary kriging interpolation to generate radar-based tropospheric refractivity maps has been studied. ECMWF's ERA5 reanalysis dataset, as well as local weather stations, have been used for the performance analysis and validation of the proposed method. The obtained results, which are summarised in Table I, demonstrate the potential of kriging interpolation to generate 2-dimensional refractivity maps from radar data, even in scenarios with a relatively low number of radar-based refractivity samples. In the case of larger areas, or areas with a complicated orography, where a spatial trend of the refractivity could be observed, universal kriging interpolation instead of ordinary kriging may be considered.

Nonetheless, it is important to point out that significant variability of the RI index used to determine the stationarity of the targets has been observed over the months. Since these changes in the stationarity of the targets might affect the accuracy of the radar-derived refractivity estimates, some sort of periodic evaluation of the quality of the stationary targets being used should be considered. In addition, even though the use of a simple k-means grouping algorithm has demonstrated good results, it would be of interest to conduct a more thorough investigation in order to optimise the clustering of the stationary targets.

ACKNOWLEDGEMENTS

The authors would like to thank the Met Office for providing both radar and local weather-station data, and the ECMWF for the open access meteorological reanalysis data. This work has been partially funded by MCIN/AEI/10.13039/501100011033 and NextGenerationEU/PRTR under project TED2021-130056B-I00.

REFERENCES

[1] J. Sun, "Convective-scale assimilation of radar data: progress and challenges." *Quarterly Journal of the Royal Meteorological Society.*, vol. 131, pp. 3439–3463, July 2005.

[2] T. Montmerle, A. Caya, and I. Zawadzki, "Short-term numerical forecasting of a shallow storms complex using bistatic and single-doppler radar data," *Weather and Forecasting*, vol. 17, no. 6, pp. 1211–1225, 2002.

[3] L. Besson, O. Caumont, L. Goulet, S. Bastin, L. Menut, E. Bresson, N. Fourrie, F. Fabry, and J. Parent du Chatelet, "Comparison of real-time refractivity measurements by radar with automatic weather stations, AROME-WMED and WRF forecast simulations during SOP1 of the HyMeX campaign," *Quarterly Journal of the Royal Meteorological Society.*, vol. 142, pp. 138–152, August 2016.

[4] WMO. (2023) Observing Systems Capability Analysis and Review. [Online]. Available: https://space.oscar.wmo.int/variables/view/air_specific_humidity_near_surface

[5] E. R. Kursinski, G. A. Hajj, W. I. Bertiger, S. S. Leroy, T. K. Meehan, L. J. Romans, J. T. Schofield, D. J. McCleese, W. G. Melbourne, C. L. Thornton, T. P. Yunck, J. R. Eyre, and R. N. Nagatani, "Initial results of radio occultation observations of earth's atmosphere using the global positioning system," *Science*, vol. 271, pp. 1107–1110, 1996.

[6] F. Fabry, C. Frush, I. Zawadzki, and A. Kilambi, "On the extraction of near-surface index of refraction using radar phase measurements from ground targets," *Journal Atmospheric and Oceanic Technology.*, vol. 14, pp. 978–987, August 1997.

[7] F. Fabry, "Meteorological value of ground target measurements," *Journal Atmospheric and Oceanic Technology.*, vol. 21, pp. 560–573, 2004.

[8] T. M. Weckwerth, C. R. Pettet, F. Fabry, S. Park, M. A. LeMone, and J. W. Wilson, "Radar refractivity retrieval: validation and application to short-term forecasting," *Journal of Applied Meteorology.*, vol. 44, pp. 285–300, March 2005.

[9] J. C. Nicol, A. Illingworth, and K. Bartholomew, "The potential of 1h refractivity changes from an operational c-band magnetron-based radar for numerical weather prediction validation and data assimilation," *Quarterly Journal of the Royal Meteorological Society.*, vol. 140, pp. 1209–1218, March 2014.

[10] D. Bodine, D. Michaud, R. D. Palmer, P. L. Heinselman, J. Brotzge, N. Gasperoni, B. L. Cheong, M. Xue, and J. Gao, "Understanding radar refractivity: Sources of uncertainty," *Journal of Applied Meteorology and Climatology.*, vol. 50, pp. 2543–2560, June 2011.

[11] B. L. Cheong, R. Palmer, C. D. Curtis, T. Y. Yu, D. S. Zrnic, and D. Forsyth, "Refractivity retrieval using the phased-array radar: First results and potential for multimission operation," *IEEE Transactions on Geoscience and Remote Sensing.*, vol. 46, pp. 2527–2537, 2008.

[12] J. Parent du Chatelet, C. Boudjabi, L. Besson, and C. O., "Errors caused by long-term drifts of magnetron frequencies for refractivity measurement with a radar: Theoretical formulation and initial validation," *Journal Atmospheric and Oceanic Technology.*, vol. 29, pp. 1428–1434, April 2012.

[13] J. C. Nicol, A. Illingworth, T. Darlington, and M. Kitchen, "Quantifying errors due to frequency changes and target location uncertainty for radar refractivity retrievals," *Journal Atmospheric and Oceanic Technology.*, vol. 30, pp. 2006–2024, April 2013.

[14] R. D. Roberts, F. Fabry, P. C. Kennedy, E. Nelson, J. Wilson, N. Rehak, J. Fritz, V. Chandrasekar, J. Braun, J. Sun, S. Ellis, S. Reising, T. Crum, L. Money, R. Palmer, T. Weckwerth, and P. S., "REFRACTT_2006: Real-time retrieval of high-resolution low-level moisture fields from operational NEXRAD and research radars," *Bulletin American Meteorology Society.*, vol. 89, pp. 1535–1548, October 2008.

[15] R. N. López, B. Sánchez-Rama, V. Santalla del Río, S. Barbosa, P. Narciso, R. Pérez-Santalla, A. Pettazzi, P. Pinto, S. Salsón, and T. Viegas, "Refractivity and refractivity gradient estimation from radar phase data: A least squares based approach," *IEEE Transactions on Geoscience and Remote Sensing*, vol. 61, pp. 1–14, 2023.

[16] N. Cressie, "Spatial prediction and ordinary kriging," *Mathematical geology*, vol. 20, no. 4, pp. 405–421, 1988.

[17] ——, *Statistics for spatial data*. John Wiley & Sons, 2015.

[18] ECMWF. (2023) ERA5 hourly data on pressure levels from 1959 to present. Copernicus Climate Change Service (C3S) Climate Data Store (CDS). [Online]. Available: https://doi.org/10.24381/cds.bd0915c6

[19] J. Li and A. D. Heap, *A review of spatial interpolation methods for environmental scientists*. Geoscience Australia Canberra, 2008.

[20] Met Office. (2023) Met Office Rain Radar Data from the NIMROD System. NCAS British Atmospheric Data Centre. [Online]. Available: http://catalogue.ceda.ac.uk/uuid/82adec1f896af6169112d09cc1174499

[21] ——. (2023) Met Office MIDAS Open: UK Land Surface Stations Data (1853-current). [Online]. Available: https://catalogue.ceda.ac.uk/uuid/dbd451271eb04662beade68da43546e1